Proceedings of the ASME 2010 3rd Joint US-European Fluids Engineering Summer Meeting and 8th International Conference on Nanochannels, Microchannels, and Minichannels
FEDSM-ICNMM2010
August 1-5, 2010, Montreal, Canada

FEDSM-ICNMM2010-30276

NUMERICAL STUDIES ON NON-BOILING TWO-PHASE FLOWS IN MICROTUBES AND MICROCHANNELS: A REVIEW

V. Talimi[1]
Faculty of Engineering and Applied Science
Memorial University of Newfoundland
St. John's, NL, Canada, A1B 3X5

Y. S. Muzychka[2]
Faculty of Engineering and Applied Science
Memorial University of Newfoundland
St. John's, NL, Canada, A1B 3X5

ABSTRACT

Numerical studies on the hydrodynamic and heat transfer characteristics of two-phase flows in small tubes and channels are reviewed. These flows are gas-liquid and liquid-liquid slug flows. The review is categorized into two groups of studies: circular and non-circular channels. Different aspects such as slug formation, slug shape, flow pattern, pressure drop and heat transfer are of interest. According to this review, there are some large gaps in the research literature, including pressure drop and heat transfer in liquid-liquid slug flows. Gaps in research are also found in applications of non-circular ducts, pressure drop and heat transfer in meandering microtubes and microchannels for both of gas-liquid and liquid-liquid two-phase flows.

Keywords: Numerical simulation, slug flow, two-phase flow, microtubes, microchannels, pressure drop, heat transfer

NOMENCLATURE

A	=	Area (m^2)
Bo	=	Bodenstein Number (Ud/D)
C	=	Fraction Function
Ca	=	Capillary Number ($\mu U/\sigma$)
C_p	=	Specific Heat (kJ/kgK)
D	=	Diameter (m)
D_h	=	Hydrodynamic Diameter (m)
Eo	=	Bond or Eotvos Number ($(\rho_G-\rho_L)gd^2/\sigma$)
Fr	=	Froude Number (U^2/Lg)
h	=	Convection Heat Transfer Coefficient (W/m^2K)
Kn	=	Knudsen Number (Λ/L)
k	=	Conduction Heat Transfer Coefficient (W/mK)
L	=	Length (m)
M	=	Morton Number ($We^3/FrRe^4$)
N_f	=	Inverse Viscosity Dimensionless Number
Nu	=	Nusselt Number (hD/k)
P	=	Pressure (Pa)
Pe	=	Peclet Number ($U_b w/D$)
Pr	=	Prandtl Number ($C_p\mu/k$)
Re	=	Reynolds Number ($\rho U D_h/\mu$)
T	=	Temperature (K)
t	=	Time (s)
U	=	Velocity (m/s)
W	=	Width (m)
We	=	Weber Number ($\rho U^2 L/\sigma$)

Greek Symbols

δ	=	Film Thickness (m)
Λ	=	Molecular Mean Free Path (m)
μ	=	Viscosity ($N.s/m^2$)
ρ	=	Density (kg/m^3)
σ	=	Surface Tension (N/m)
Φ	=	Distance to the Interface

Subscripts

L	=	Liquid
G	=	Gas
GB	=	Gas Bubble

INTRODUCTION

Enhancement in heat transfer at small scales is an active area of study followed by many researchers. Using two-phase non-boiling flows including plug/slug flows or Taylor flows has become a very interesting method for achieving higher cooling capacities. Most of the researchers have studied this area experimentally. As a result of this and many other reasons, there are significant gaps in areas analyzed using numerical simulations. One of the most important reasons can be the time-expense of the numerical methods. Numerical simulation as a method for predicting the heat and mass transfer characteristics has gained popularity due in part to the developments in the

[1] Corresponding author, e-mail: v.talimi@mun.ca
[2] e-mail: y.s.muzychka@mun.ca

computational hardware and software. In the present review, the various numerical studies on simulating non-boiling two-phase flows in small (mini and micro) scales is examined. Much of the work conducted done in recent years has been reviewed and the results gathered and categorized into two major areas. These sections include circular or non-circular channels and gas/liquid or liquid/liquid two-phase flows.

General Notes

One of the initial and important steps in numerical simulation of a fluid flow is to examine whether laminar or turbulent conditions exist. The critical Reynolds number corresponding to the onset of turbulence is 2300 for liquid flow in tubes with diameters as small as 50 µm [1]. Another critical *Re* has been reported to 1000 for single moving droplets [2].

In mini and micro scales the interaction between two fluids at their interface can be important. The importance of surface tension effects is determined based on the Reynolds number *Re* and capillary number *Ca*; or *Re* and Weber number *We*. For *Re* << 1, the quantity of interest is *Ca* and for *Re* >> 1 the quantity of interest is *We*. Surface tension effects can be neglected if *Ca* >> 1 or *We* >> 1. [3]

In order to decide whether the no slip assumption is valid or not, especially for the flow of gases at small scales, one should use the Knudsen number *Kn*. The *Kn* criteria for different flow regimes are as follows [4]:

$0 < Kn < 0.001$	Continuum flow
$0.001 < Kn < 0.1$	Slip flow
$0.1 < Kn < 10$	Transition flow
$Kn > 10$	Free molecular flow

The commonly solved equations of motion are for incompressible flows, i.e. the continuity equation, the momentum equation and the energy equation:

$$\nabla.\vec{U} = 0 \tag{1}$$

$$\rho \frac{D\vec{U}}{Dt} = \rho\vec{g} - \nabla P + \mu\nabla^2\vec{U} \tag{2}$$

$$\rho C_p \frac{DT}{Dt} = k\nabla^2 T + \dot{s} \tag{3}$$

In order to simulate the interface between two phases there are two major methods applied in the solution: the Volume of Fluid (VOF) method and the Level Set method (LS). The VOF method is based on the idea of the so called fraction function “C”. Basically, when the cell is empty (no trace of fluid inside) the value of C is zero, if the cell is full, we have a value for C = 1, and when the interface of two phases cuts the cell, then 0 < C < 1. The equation to be solved is [6]:

$$\partial_t C + U.\nabla C = 0 \tag{4}$$

The most popular approach used to solve the above equation is “geometrical reconstruction”, originating in the works of Hirt and Nichols [6].

In the LS method, the interface between immiscible fluids is represented by a continuous function Φ. This function represents the distance to the interface, and equals to zero on the interface, has a positive value on one side of the interface, and a negative value on the other side. This way both fluids are identified, such that the location of the physical interface is associated with the zero level. The LS equation is as follows [7]:

$$\partial_t \Phi + U.\nabla\Phi = 0 \tag{5}$$

Material properties such as the density, the viscosity, the heat capacity and the thermal conductivity are updated locally based on Φ, and smoothed across the interface using a smooth Heaviside function.

Eulerian and Lagrangian Viewpoints

There are two viewpoints commonly used by researchers for analyzing fluid motion. In the first one, the Eulerian viewpoint, all of the necessary properties such as density, pressure, velocity and temperature have to be completely determined as functions of space and time. On the other hand, by using the Lagrangian viewpoint, one can focus on an individual fluid particle or droplet as it moves about and express any variable in terms of four independent variables x, y, z, and t in order to indicate location and time. In other words, in this method a moving frame of reference is used.

Many researchers have used the Eulerian viewpoint to simulate two-phase flows in micro tubes and microchannels [8 to 15]. They mainly set up the computational domain as showed in Fig. 1 with some differences. In this way, one should consider the minimum ratio of length to diameter (L/D) or length to width (L/W) of domain to let the slugs be formed and the flow become fully developed. This ratio should be at least 40 according to the various reports [16]. This long domain requires a large number of iterations specially when the heat transfer is of interest, therefore the CPU time and costs will be high. Note that the domain showed in Fig. 1 is typical and researchers may use it with some differences. For example the geometry of junction could be a T-junction [8, 14, 15], Y-junction [11, 17], nozzle type [9, 10, 12] or even premixed inflow [17]. Also some researchers used 3-dimensional domains [13, 17, 18] or curved domains [17]. The length of two-phase formation region showed in Fig. (1) is depended on many conditions like the type of the two-phase flow. This length is reported up to four diameters for bubbly flow and seven dimaters for slug flow [16].

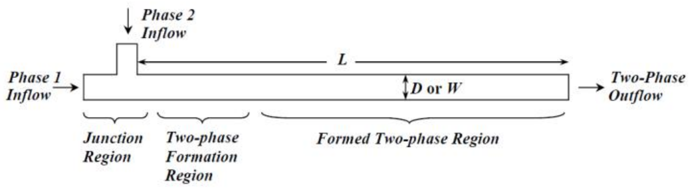

Fig. 1 – A typical computational domain frequently

used for Eulerian viewpoint

In order to increase the ease of simulation and simulation time, some researchers have used the Lagrangian viewpoint to pursue a particular part of the flow, such as a droplet or a bubble [19-23]. The typical computational domain used for this purpose is illustrated in Fig. 2. This method is appropriate for analyzing the steady state shape of a liquid slug, gas bubble shape. Similarly, the flow pattern such as internal fluid circulation and the liquid film thickness around the bubble in the gas-liquid two phase flows in microtubes and microchannels. However, it is not well suited for any case such numerical simulation of convective heat transfer in two-phase flows, because of the unsteady nature of the convection mainly caused by the slugs' relevance through the film thickness. There are some exceptions, like convective heat transfer in discrete droplets [24, 25] due to the fact that there is no relation between a droplet and the upstream and downstream droplets. Another example is the situation in which there is a dry-out condition and there is no convective mass transfer between the liquid slugs. The domain presented in Fig. 2 is typical of many studies and may used in different ways, including 3-dimensional domains [18, 20] and curved paths [23].

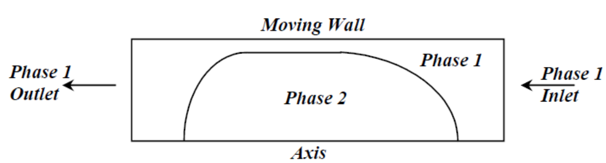

Fig. 2 – A typical computational domain frequently used

for Lagrangian viewpoint.

GAS/LIQUID FLOW IN CIRCULAR CHANNELS

Slug Formation

The process of slug formation in circular channels has been studied for different mixing zone shapes: T-junctions, Y-junctions, pre-mixed inlets, and annular inlets. The parameters of interest which have been studied by researchers are the diameter of the mixing zone, the channel curvature (for meandered channels), and superficial velocities of the two phases. The forces which have been studied by recent researchers include surface tension, viscous friction, inertial, and gravitational forces. The effects of these forces can be presented using the different dimensionless groups such as the Reynolds number, *Re,* and capillary number, *Ca*.

Shao et al. [12] reported a multistage mechanism for bubble formation that consists of expanding, contracting and necking stages. These descriptions refer to the movement of gas-liquid interface at the lower end of the bubble close to the nozzle. In the initial expanding stage, the liquid is displaced by the emerging gas, while the gas liquid interface moves away from the tube axis. As the bubble is pushed forward in the channel, the interface retracts back toward the tube axis, i.e. contracting stage. As the bubble grows further in the radial direction and starts blocking the channel, leaving only a thin liquid film close to the wall, liquid pressure builds up upstream. The lower end of the bubble is squeezed, and as a result, a neck forms that connects the bubble body with the tip of the gas nozzle. This is the necking stage, which takes place quickly as compared with the previous stages.

Qian and Lawal [8] numerically investigated the effects of some parameters such as pre-mixing level and mixing zone geometry on gas slug lengths. They reported that as the two phases (gas and liquid) are mixed better, in the inlet of microchannel the gas slug lengths become shorter (similar results were also reported by Kumar et al. [17]). They also showed that in order to achieve shorter gas slugs, it is better to introduce gas and liquid feeds head to head or perpendicular to each other with the liquid stream parallel to the microchannel. By decreasing the diameter of the mixing zone, the gas slug length decreases. Their results also showed that the gravitational effects can be ignored in microchannels because on this scale of diameter, two phase flow is influenced mainly by surface tension, viscous frictional, and internal effects. Shorter gas slugs can also be produced by decreasing the superficial velocity of gas, or increasing the superficial velocity of liquid phase. Furthermore, their study on the influence of fluid properties on slug length showed that the surface tension effect is stronger than the viscous effect, and by increasing the surface tension of the liquid, the gas slug length increases too.

Chen et al. [9] indicated that the bubble departure size (the maximum radius or diameter of growing Taylor bubbles just before their departure) in micro tubes under liquid co-flow mainly depends on liquid and gas superficial velocities. As the gas superficial velocity increases (or the liquid superficial velocity decreases), the Taylor bubble departure diameter increases. At the same time the length of Taylor bubbles increases dramatically (same results were also reported by Kumar et al. [17]).

Kumar et al. [17] also reported that by increasing the curvature ratio (the ratio of coil diameter to tube diameter) the slug length also increases for both gas and liquid phases. They proposed following the reasons for this behaviour. For low curvature ratios the small slugs formed because of the strong centrifugal forces. As the curvature ratio increases, the centrifugal force becomes weaker and slug length increases. They also showed that by decreasing, *Ca*, the gas slug length increases by showing that when surface tension increases or viscosity decreases, the gas slugs become longer.

Film Thickness

The effects of different parameters on the liquid film thickness have also been studied. These parameters are Ca, Re, Fr, bubble length, and flow direction (with gravitational effects).

Gupta et al. [10] compared the numerically calculated liquid film thickness with different empirical correlations and showed that the best agreement is with Betherton's prediction [26]:

$$\frac{\delta}{D_h} = 0.66 Ca^{2/3} \tag{6}$$

This equation is applicable for $Ca \ll 1$.

Chen et al. [9] calculated the liquid film thickness around the bubble for different *Ca,* and compared their results with the Bretherton correlation. They argued since the bubble length in their study was smaller than three times the micro tube diameter, the results show some difference from Bretherton's prediction.

Taha and Cui [21] reported on the independence of liquid film thickness around a rising bubble in vertical micro tubes having a diameter on the order of the bubble length.

Edvinsson and Irandoust [27] (and also Taha and Cui [28]) showed that the liquid film thickness increases with Ca, Re and Fr. They argued that for small microchannels it is sufficient to correlate the liquid film thickness with Ca. As flow rates and diameters increase, the effects of inertial forces as well as gravitational forces become more pronounced.

Flow Patterns

Bubble length, *Pe*, *Bo*, *Ca*, pressure gradient, flow direction (gravitational effects), channel curvature (for curved microchannels), and superficial velocities of the two phases have been reported as the effective factors on the flow patterns and therefore mass transfer by many researchers. Another important factor is whether the bubble touches the channel walls, i.e. dry-out condition, or not.

Muradoglu et al. [19] studied the effects of *Pe* on the axial mass transfer (dispersion) in the liquid slugs. They found that "convection" is the main parameter that controls the axial dispersion through the liquid film at small values of *Pe*. On the other hand, "molecular diffusion" between the re-circulating vortices and the film region is the most prominent parameter that controls the axial dispersion for large values of *Pe*. They introduced three different regimes of *Pe*:

(1) Convection-controlled regime when $Pe > 10^3$
(2) Diffusion-controlled regime when $Pe < 10^2$
(3) Transition regime when $10^2 \leq Pe \leq 10^3$

Salman et al. [31] investigated numerically the effect of axial mixing in liquid phase of Taylor flows for low *Bo,* where diffusion is sufficiently large, and reported an increase in axial mixing of the tracer particles in liquid slugs with increasing *Ca* and argued this is because of a thicker liquid film around the bubbles and better communication between slugs. They also showed that axial mixing increases with increases in bubble and slug length. They suggested using short bubble and slug lengths in order to have reduced axial mixing.

He et al. [29] found that for Taylor flow when the wall is perfectly wetted by liquid, the gas bubble to liquid velocity ratio is approximately 1.2, which agrees well with the Armand correlation [32] but when the gas bubbles contact with the wall directly i.e. a dry-out patch, the gas bubble flows with the same velocity as liquid slugs.

Ua-arayaporn et al. [30] reported higher ratios of gas velocity to liquid velocity for higher pressure gradients and argued this is because the change of bubble shape for higher pressure gradients. At higher pressure gradients, the bubble is elongated in the central region of tube or pipe and less influenced by the no-slip wall condition.

Edvinsson and Irandoust [27] argued that for small microchannels it is sufficient to correlate the relative velocity of gas plugs with *Ca*. As flow rates and diameters increase, the effects of inertial forces as well as gravitational forces become more pronounced. In addition, the size of the recirculation vortices within the liquid plug decreases rapidly with increases in liquid film thickness.

Narayanan and Lakehal [33] focused on the effect of gravity on the breakup into slugs and according to their results, the slug breakup happens slightly earlier for up-flow, which leads to a higher breakup frequency.

Fries and Rohr [23] showed that the symmetrical velocity profile, known from straight microchannels, changes to an asymmetrical one for the meandering channel configuration. This change leads to an enhanced radial mass transfer inside the liquid slug, resulting in a reduced mixing length. Besides, smaller radius of curvature provides more mixing rather than larger radius of curvature microchannels. They argued this is because of larger centrifugal forces. For meandering channel designs, on one hand, longer slug lengths provided an enhanced mass transfer due to the bending angle of the slug. On the other hand, shorter liquid slugs have smaller turning angles than longer slugs, providing an enhanced asymmetrical flow pattern. According to their discussion, the optimal slug length for fast mixing depends on the bend geometry.

Taha and Cui [28] reported that at low *Ca*, the shape of streamlines at both ends of the bubble are nearly identical and close to the bubble ends, streamlines bow sharply to complete the vortex path. They also mentioned that this localized effect of the bubble can be seen only within a bubble diameter from the bubble nose. They also showed that as *Ca* increases, the vortices in the liquid plug become smaller and the radial position of the vortex centers shift toward the capillary axis. Also, by increasing *Ca*, the liquid film flowing around the bubble as well as liquid film thickness increases, and complete bypass flow occurs around Ca=0.5. They observed two stagnanation points in the liquid plug: one on the bubble tip and the second inside the liquid plug.

Ilnicki et al. [34] reported that for high values of overall velocities (U_G+U_L>0.4 m/s) the time necessary to reach a steady Taylor flow increases significantly if the slip ratio (U_G/U_L) is higher than 1. On the other hand, for the overall velocities lower than 0.4 m/s this necessary time increases only if the slip ratio is higher than 2.5.

Carlson et al. [35] reported some differences between the numerical results obtained by Fluent™ and TransAT™ in the cases of bubbly and slug flows inside micro tubes. They pointed out that a recirculation flow was predicted inside the bubbles in bubbly flow by TransAT™ but Fluent™ did not show any significant circulation inside bubbles. Besides, in the case of slug flow, TransAT™ predicted a periodic slug formation but not in Fluent™. According to their report, TransAT™ predicted the results closer to the experimental results in this case.

Bubble Shape

Typically, a Taylor bubble has a sharp front nose and a relatively flattened bottom. The liquid film formed between the bubble and the wall is uniform at the middle portion. The film thickness of the liquid around the gas bubble increases continuously towards the front nose (as it has been showed schematically in Fig. 2), while it shows somewhat wavy behavior towards the bottom portion.

Taha and Cui [21] found that by decreasing the Morton number, *M*, under a constant value of Eotvos number, *Eo*, the bluntness of the bubble nose increases and the bubble tail flattens, which results in an increment of the liquid film thickness around the bubble. Also the bluntness of bubble nose increases as *Eo* goes up.

Chen et al. [9] reported a change in the front and rear shapes of the departed Taylor bubbles with *Re* (defined based on the two-phase velocity $U=U_L+U_G$). Based on their results, at low *Re*, both the front and rear sides of Taylor bubbles show a hemispherical cap shape. As *Re* increases, the curvature radius of the bubble tip become smaller and the rear cap becomes flattened. They also showed that when the liquid superficial velocity is small enough when compared to the gas superficial velocity, long Taylor bubbles can be formed by merging a growing bubble with the departed Taylor bubble in front of it. This approach is called Taylor-pairing or doubling. They also reported a very prominent result in their work. They showed that under the same liquid and gas superficial velocities, the size of Taylor bubbles inside a given geometry of micro tube can vary distinctly for different bubble generation devices. In other words, for a given set of U_L and U_G, different flow patterns can occur inside the same channel.

Edvinsson and Irandoust [27] showed that as *Ca* increases, the convexity of the rear side of bubble lost and then inverted. They also reported that as *Re* increases, a multiple wavelet has formed in the film near the rear side of the bubble and its amplitude increases with *Re*.

Shao et al. [12] argued that because of changes in the bubble length, the length of the bubble just after formation is not constant and would not be representative of the size. According to their results, the bubble size increases with increasing gas and decreasing liquid superficial velocity. Also, bubble size is mainly affected by surface tension and only slightly by density and viscosity. They reported an increase in bubble size with increasing nozzle size, and argued the reason as follows. For the same gas flow rate, the gas flux in the large nozzle, which has a detaching effect, decreases. In addition, the increased periphery of the large nozzle increases the surface tension force, which has an attaching effect. Both help to expand the bubble formation time and thus its size.

Ua-arayaporn et al. [30] studied the shape of bubbles in a slug flow through micro tubes and found that the bubbles are nearly spherical under the weak pressure gradients.

Taha and Cui [28] reported spherical Taylor bubble ends at low *Ca* and nearly identical streamlines at both ends of the bubble. They also showed that as *Ca* increases, the bubble nose becomes more slender and liquid film flowing around the bubble is thicker. They discussed three separate regions in the leading edge of the bubble: the bubble cap region, the liquid film region and the transition region between them. According to their results, increases in *Ca* results in an increase of the liquid film thickness and the sharpness of the bubble nose. This results in smaller bubble caps and larger transition regions.

Pressure Drop

Pressure drop in two-phase flows inside circular micro channels has been studied as a function of slug length, bubble length, bubble frequency, and *Ca*. Also, some researchers have noticed the effects of curvature and channel width for two-phase flows inside meandering microchannels.

Chen et al. [9] showed that with decreasing slug length or increasing bubble length, the friction factor increases quickly. Therefore, in order to reduce the pressure drop, the larger nozzle (for dosing gas into the liquid to make Taylor bubbles) has to be used, from which longer bubbles are generated.

Gupta et al. [10] showed that in a computational unit cell consisting of a Taylor bubble and two half liquid slugs ahead and behind the bubble, the pressure distribution along the axis in the bubble is constant and higher than that of the liquid phase. They also reported that the pressure distribution in the liquid region ahead of the bubble has a monotonic decrease with distance, which is consistent with the developing flow, and a more complex pressure distribution in the liquid phase behind the bubble because of the numerical effects.

He et al. [29] reported that for a dry-out two-phase flow condition where there is no liquid film around the gas phase, higher frequency of bubbles induces more circulations in liquid slugs and increases the pressure drop.

Fries and Rohr [23] assumed two-phase flow in meandering microchannels and reported that pressure drop of the gas-liquid Taylor flow increases when channel curve radius and channel width decrease.

Lakehal et al. [16] reported an increase of 14-15% in pressure drop of slug flow with $L_{GB}/L=5.14$ compare with a single phase flow. According to the results of Ua-arayaporn et al. [30] this increase in pressure drop is due to the circulation region in the liquid slugs.

Taha and Cui [28] observed the fluctuations in the wall shear stress ahead of and behind the slug, and nearly zero pressure drop in the central region. They also reported that the pressure drop across the bubble front increases with increasing *Ca*, and that surface tension induced stresses are dominant at small *Ca*.

Heat Transfer

Several researchers (He et al. [29], Lakehal et al. [16,33], Ua-arayaporn et al. [30]) reported notably higher *Nu* in two-phase gas-liquid slug flows in micro tubes compared with single phase flows. According to the literature, slug length and gravity has effects on the heat transfer.

He et al. [29] reported that the wall temperature locally peaks when a gas bubble passes. According to their results the local *Nu* is large beneath the bubble with a liquid film and that the liquid film between gas bubble and wall significantly increases the local *Nu*. They also argued that the circulation within the liquid slug, is the primary mechanism of enhancement in the heat transfer.

Lakehal et al. [16] argued that there are two separate heat transfer regions in gas-liquid slug flow in micro tubes: one right at the initial breakup and one far downstream in the fully developed region. In the first region, the thermal boundary layer is compressed by the rear of bubble and this promotes locally the radial temperature gradient and heat transfer along the micro tube. In the second region, the main heat removal mechanism is seen to be essentially a convective transport, taking place at the back of the slug where a jet-like flow forms and penetrates the cell and transports heat into the core. According to their results, there is a substantial increase in *Nu* with increases in the gas bubble length L_{GB}. For $L_{GB}/L=5.14$ the mean *Nu* reached a value of 17.20 for the fully developed region which is much greater than 3.67 for single phase heat transfer in a microchannel having a constant wall temperature boundary condition.

Ua-arayaporn et al. [30] showed that in a slug flow, *Nu* increases notably in the region where the bubble exists. They argued this is because of the small difference between local bulk and wall temperatures.

Nrayanan and Lakehal [33] reported a substantial increase in heat transfer rate with increasing gas slug length. They obtained an average *Nu* of 15 for slug flows and indicated that using slug flows may lead to an overall enhancement in heat transfer by a factor between 3 and 4 compared to single-phase flows is attainable. They also showed that gravity has some effects on heat transfer in slug flows, and in particular the down-flow case where the direction of gravity is the same as direction of flow, the average *Nu* is about 4% higher compared to the zero gravity cases. They argued that an additional shear created by the perturbation flow field in slug flows is responsible for increasing the heat transfer rate in two-phase flow.

LIQUID/LIQUID FLOW IN CIRCULAR CHANNELS

Slug Formation

The effects of a small number of parameters on the slug formation process in liquid/liquid flows have been studied in the recent years. These parameters are wall adhesion, wall confinement, and *Ca*.

Kashid et al. [11] simulated slug formation in a Y-junction mixer using two liquids and reported that the wall adhesion plays a very important role in formation of the plugs. According to their unsteady simulation results, the two liquids travel through a Y-junction as two parallel flows to a certain distance and due to wall adhesion the interface makes an angle with the wall and thus slug formation takes place.

Chung et al. [36] reported a very weak dependency of drop deformation on the wall confinement although the drop deformation is known to increase as wall confinement ratio increases. They also reported that as *Ca* increases the drop is more aligned with the flow direction.

Wu et al. [14] showed that the distance between two neighboring droplets increases with a decrease in *Ca*. At the same time, the size of the generated droplets also increases when *Ca* decreases. At small *Ca*, the droplet diameter becomes larger than the width of the channel and slugs are generated. On the other hand, at larger *Ca*, the influence of the channel geometry decreases due to the smaller droplets generated, which do not touch the channel walls.

Flow Patterns

Kashid et al. [11, 37-39] have carried out a number of numerical simulations on the flow pattern inside the slugs. The effect of different parameters including *Re*, interface shape, and circulation intensity were of interest in their works. The effects of *Ca* and *We* were also studied recently [14].

Kashid et al. [11] performed numerical simulations for a liquid-liquid plug flow in micro tubes considering two liquid plugs separately. They considered two cases for the second liquid plug: with and without a thin film around the computational domain. According to their results two flow patterns exist in each slug: a recirculation zone at the center and in the wall proximity and two stagnant zones in between them. Thus, there is a parabolic velocity profile showing the maximum velocity at the center of the slug, zero velocity at some radial position and negative velocity at the wall surface.

Kashid et al. [37] showed that in liquid-liquid flows, both of the slugs show similar velocity profiles though the viscosities were different, and argued this is due to very low *Re* in which the flow is still under Stokes flow regime where the velocity profiles are independent of viscosity. They also reported the enhancement in mass transfer due to recirculation in the slugs.

Kashid et al. [38] mentioned that convective mass transfer takes place to a degree, depending on the intensity of internal circulations, while inter-phase mass transfer depends on the intensity of flow at the ends of both slugs. For liquid slugs with lengths greater than their diameters, the radial position of the stagnant zones are located at roughly half the micro tube radius and shift slightly toward the center of the slug with increasing liquid flow velocity. On the other hand, for shorter slugs, the dimensionless radial position of the stagnant zones located between the center of the slug and the walls at low velocities and goes towards the center rapidly, with increasing velocity. They also reported that in the case of a slug without film and a length longer than its diameter, the flow velocity has no significant effect on the normalized circulation time. But for the slugs with the length smaller than their diameter, at low liquid velocity, the circulation time is constant, but with an increase in the flow velocity, the circulation time decreases and subsequently remains constant.

Wu et al. [14] reported that for small *Ca*, the flow patterns are the same for different *We*. This is due to the relatively larger influence of *Ca* on the flow. But when the inlet velocity is large, the flow mode is not only decided by *Ca* but the influence of *We*, is also significant because of the squared velocity term.

Kashid et al [39] observed that there are four stagnant zones within each slug on the upper and lower parts and at the front and rear ends. According to their results, in some slugs, the stagnant rear zone does appear if the rear side is a perfect hemisphere. They also observed that increasing the average carrier velocity leads to an increase in the thermal circulation within the slugs.

GAS/LIQUID FLOW IN NON-CIRCULAR CHANNELS

Slug Formation

Ghidersa et al. [18] mentioned that the generally accepted minimum value of the *Ca* for which the bubble shape remains axisymmetric i.e. the bubble cross section at any axial position is circular, is 0.04. According to their results, the bubble shape remains circular even up to *Ca* = 0.043, which they argued is in agreement with other published studies.

Film Thickness

The effects of different parameters including *Ca*, gravity effects, channel shape and geometry, and bubble length on the thickness of liquid film around the bubble has been of interest in recent research.

Ghidersa et al. [18] reported that the liquid film thickness around the Taylor bubbles increases with increases in the *Ca*.

Taha and Cui [22] showed that there is a difference between the liquid film thickness for upward and downward flows in square microchannels, for *Ca* = 0.009. For this low *Ca*, the liquid film thickness deposited at the walls for upward flow was thicker than the downward flow because of gravity forces.

Onea et al. [40] considered a cylindrical bubble in a square mini-channel and did the same simulation in a rectangular mini-channel with the same hydraulic diameter and flow parameters. They showed that the bubble in the square channel has a circular cross section while in the rectangular channels the bubble is squeezed between the long walls. Therefore, the thickness of the liquid film relative to the smaller dimension is decreasing while the other is increasing.

Liu and Wang [13] reported a thinner liquid film thickness at the side walls in equilateral triangular microchannels as compared with square microchannels for the same hydraulic diameters and initial volume of Taylor bubbles. They also showed that liquid film thickness in square microchannels is less than circular micro tubes in whole range of *Ca*. They presented the reasons as follows. The symmetry of the circular microchannel lead to a uniform liquid film between Taylor bubbles and the wall, but in square and equilateral triangular microchannels most of the liquid is squeezed into the corners which results in thinner liquid films on side walls.

According to Yu et al. [15], the liquid film around the bubbles could become very thin or even partially dry-out in small channels with width of around 50 micrometers. The film thickness depends on the magnitude of the surface tension, the bubble length, the bubble velocity and the surface property.

Velocity and Flow Patterns

According to the recent reports, velocity field and flow patterns are affected by *Ca*, channel shape and geometry, slug length, and local pressure gradient. There is also a reported critical *Ca* in which a complete bypass occurs. This critical value has been reported for a few channel shapes such as squares and triangles.

Worner et al. [20] reported that the velocity profile in the liquid slug has the same parabolic form for different lengths of computational domain.

Taha and Cui [22] showed numerically that the behavior of dimensionless bubble velocity of Taylor flow in square microchannels is similar to circular micro tubes, except for low *Ca* where it increases with *Ca*. They also showed that the transition to complete bypass occurs around *Ca*=0.4. According to their results, there are two obvious and separate vortices ahead of and behind the bubble at low *Ca*. As *Ca* increases, similar to the circular micro tubes, the eye of vortices moves away from walls and shifts toward the symmetry line. At high *Ca*, recirculation regions vanish and there is a complete bypass. They showed that the liquid flow field is absolutely not axisymmetric at low *Ca* by presenting two different positions of the vortex eye from the side and diagonal views.

Onea et al. [40] reported that liquid slug length impacts on mass transfer so short liquid slugs are good for obtaining a large increase in mass transfer in the liquid phase, within a short time interval, and long slugs were suggested for use for applications where the target is mass transfer from gas bubble into the liquid phase. They also did their simulations for rectangular geometries with different aspect ratio, but having the same hydraulic diameter. According to their results, as the aspect ratio of the channel increases, more mass is transferred in the liquid phase.

Ghidersa et al. [18] reported that for the cross section with the smallest film thickness, in the liquid film surrounding the bubble a back flow region has been found. They argued this flow corresponds to a local high positive pressure gradient due to the rapid change in film thickness.

Liu and Wang [13] like other researchers [22, 41] reported that with increases in *Ca*, the distribution of the vortex centers transferred from square and equilateral triangular shapes across the channel into the circle gradually, and become smaller and smaller. They argued that as the vortex centers shifted toward the centerline, more liquid flows toward the bubble and forms a thicker film thickness. Finally at critical *Ca*, at which the bubble velocity is equal to the maximum liquid velocity, there is a complete bypass and no circulation in liquid plug. They obtained a critical *Ca* of 0.8 and 1.0 in square and equilateral triangular shapes, respectively.

Bubble and Interface Shapes

The main parameters, which have strong effects on the bubble shape and interface between two phases, are *Ca* and superficial velocity ratio.

Taha and Cui [22] performed a numerical simulation on bubble shape for different flow parameters in square microchannels and found that the shape of bubbles depends strongly on *Ca* number. According to their results, at low *Ca*, the bubbles are not axisymmetric and flatten out against the walls. Also, both the front and rear ends of the bubbles are spherical. When *Ca* increases, the bubble end loses its spherical shape and after a while the curvature of the bubble end reverses. In other words, convex bubble end is converted into a concave bubble end. As the *Ca* number increases, the bubble becomes longer and more cylindrical. At higher *Ca* numbers, we have cylindrical bubbles. There are several different reports on transition *Ca* limit from 0.1 to 0.04 [22,41].

Liu and Wang [13] carried out a numerical study on bubble shape with respect to *Ca* through square and equilateral triangular microchannels. They also argued as other researchers [22,41], that interface shape depends on *Ca* number and because the liquid film thickness in corners is larger than side walls, the liquid flows more slowly in the corners and the pressure field is shaped by the contribution of the viscous force, inertial force and surface tension. They also reported the transition *Ca* limit of 0.1 for square microchannels and discussed two potential causes for differences between this limit and the value of 0.04 reported by other researchers. Firstly, the inertial effect was considered in their study and second, they simulated a finite long bubble in their work.

Yu et al. [15] reported that larger gas to liquid flow ratio leads to longer gas bubbles. Also, under the same flow rate ratio, a smaller *Ca* number yielded a longer bubble. They also mentioned that for a very low *Ca* (Ca < 0.01) the bubbles usually pinched off by the pressure difference in the two phases, and presented in slug form. According to their results, the geometry of the mixing section also affects the bubble size and the spacing between the bubbles.

Reznik and Yarin [42] simulated numerically the change in the contact angle of a droplet squeezing between two moving walls and reported that the free surface deviates from circularity at the beginning of the squeezing process and after sufficiently strong squeezing, the contact angle gradually goes up toward the value of π. According to their results, the free surface becomes more similar to the circular shape during the final steps of squeezing.

Pressure Drop

The pressure drop or wall shear stress for the slug flow inside non-circular channels were not studied extensively and only the effects of *Ca* and flow direction (gravity effects) were on interest in recent years.

Taha and Cui [22] investigated numerically wall shear stress for Taylor flow in square microchannels for two directions (upward and downward) and according to their results the side wall shear stress distributions are the same for both flow directions at low *Ca*. They also showed that similar to circular capillaries at low *Ca*, there are some fluctuations in shear stress profile and that the central region of the profile (related to bubbles body) has near-zero value. They argued that the corner wall shear stress for upward flow is higher than the downward flow, because of the different liquid film thickness in these two cases.

Heat Transfer

The prominent parameters which affect heat transfer in non-circular channels have been reported as *Pe*, slug length, channel geometry, interface shape (contact angle), and flow pattern (internal circulations). The usual assumed channel shape in the literature has been two parallel plates.

Baird et al. [24] showed that shorter droplets moving between two parallel plates have higher values of *Nu* and as the length of the droplets increases the heat transfer characteristics moves toward the single phase heat transfer, because the main mechanism of increasing convective heat transfer i.e. internal circulations in the droplet has less effect. They also mentioned that there are additional important parameters in Digitized Heat Transfer (DHT) rather than conventional single phase cooling flows including the *Pe* number, the droplet length, the distance between two parallel plates, and the meniscus curvature effects. As a result, the plots of *Nu* versus position of droplets should include all of the aforementioned parameters.

Young and Mohseni [25] reported that *Nu* achieved a greater value (after initially oscillating) for any droplet size compare with continuous Graetz flow. They argued this is because of the circulating internal flows within the droplets that help to achieve better convective heat transfer. They also showed that as the droplets become shorter, the *Nu* increases because there is relatively more cool fluid inside the droplet that can be brought into contact with the heated wall in comparison to the longer droplets. They reported that *Nu* begins to decline (before being constant) because the fluid, which has previously been heated, completes its circulation and is brought back to the heated walls. They also reported a locally higher value of *Nu* before stabilization. They presented the reason as follows. For a longer droplet, the majority of the heat diffusion occurs in the wall-normal direction. As the droplets become shorter, diffusion in the wall-tangent direction plays a growing role. When these two diffusion times are near equal in magnitude, the highest peak in *Nu* is achieved.

Oprins et al. [43] studied numerically the internal flow patterns and heat transfer inside electrostatic actuated droplets moving between two parallel plates. They carried out steady and time-dependent simulations, assumed laminar flow and constant fluid properties. They also proposed a lumped model by dividing the droplet into four cells for steady state case, and then expanded it in order to make it capable of predicting unsteady heat transfer inside the moving droplet, before it becomes thermally saturated. They reported that the heat transfer increases to twice that as compared to the minimal heat transfer only by heat conduction in the liquid.

Sammarco and Burns [44] performed a finite difference analysis to investigate the effect of different parameters on micro-fabricated device heat transfer behavior, using a moving droplet. They suggested a new optimized value for a dimensionless parameter, which is useful in design purposes. In addition, they showed that for $Pe \leq 0.1$, one can achieve more uniform interface temperatures.

LIQUID/LIQUID FLOW IN NON-CIRCULAR CHANNELS

The liquid-liquid two-phase flows in non-circular microchannels have not been considered extensively in the numerical simulations. Only a few numbers of researchers have studied the effects of some general parameters such as *Ca* and *Re* on the slug formation process and flow patterns.

Slug Formation

Wu et al. [45] reported the strong dependence of plug size on *Ca*. They showed that (for their case) by increasing *Ca*, droplets become shorter as compared with the channel width. They also showed that for $Ca < 0.005$, only droplet length is influenced by *Ca* and that for higher *Ca*, it is influenced by both *Ca* and *Re*.

Flow Patterns

Raimondi et al. [41] categorized the liquid-liquid slug flows in square microchannels into three main categories: flow with internal vortices in both the continuous and dispersed phases and a thin film that wets the wall for *Ca* higher than 0.01, flow with several recirculation nodes in the droplets for low *Ca* and *Re*, and flow without any recirculation loops in the continuous phase for low *Ca* but high *Re*.

CONCLUSION

Numerical studies on hydrodynamic and heat transfer characteristics of gas-liquid and liquid-liquid slug flows in small tubes and channels have been reviewed. Recent developments in computer hardware, software and networks, have helped researchers to overcome many of the hardships of numerical simulations. According to this review, there are some large gaps in the numerical studies of two-phase flow in micro tubes and microchannels such as:

- Pressure drop and heat transfer of liquid/liquid slug flows especially in non-circular ducts.
- Pressure drop and heat transfer in meandering micro tubes and microchannels for both of gas/liquid and liquid/liquid two-phase flow.

ACKNOWLEDGMENTS

The authors acknowledge the financial support of the Natural Sciences and Engineering Research Council of Canada (NSERC).

REFERENCES

[1] Incropera, DeWitt, Bergman, Lavine, "Fundamentals of heat and mass transfer", 6th edition, John Wiley & Sons, 2007

[2] H. Ren, R. B. Fair, M. G. Pollack, E. J. Schayghnessy, 2002, "Dynamics of electrowetting droplet transport", *Sensors Actuators*, B **87**, pp. 201-206

[3] "Fluent 6.3 User Guide", FLUENT INC. 2006

[4] C. B. Sobhan, G. P. Peterson, 2008, "Microscale and Nanoscale Heat Transfer, fundamentals and engineering applications", CRC Press, Taylor and Francis Group

[5] H. K. Versteeg, W. Malalasekera, 1995, "An introduction to computational fluid dynamics", 1st edition, Longman Scientific and Technical

[6] C. W. Hirt, B.D. Nichols, 1981, "Volume of fluid (VOF) method for the dynamics of free boundaries", *Journal of Computational Physics,* **39** (1)

[7] M. Sussmann, P. Smereka, S. Osher, 1994, "A level set approach for computing solutions to incompressible 2-phase flow", *Journal of Computational Physics,* **114** (1) pp. 146-159

[8] D. Qian, A. Lawal, 2006, "Numerical study on gas and liquid slugs for Taylor flow in a T-junction microchannel", *Chemical Engineering Science,* **61**, pp. 7609-7625

[9] Y. Chen, R. Kulenovic, R. Mertz, 2009, "Numerical study on the formation of Taylor bubbles in capillary tubes", *International Journal of Thermal Sciences,* **48**, pp. 234-242

[10] R. Gupta, D. F. Fletcher, B. S. Haynes, 2009, "On the CFD modelling of Taylor flow in microchannels", *Chemical Engineering Science,* **64,** pp. 2941-2950

[11] M. N. Kashid, F. Platte, D. W. Agar, S. Turek, 2007, "Computational modelling of slug flow in a capillary microreactor", *Journal of Computational and Applied Mathematics,* **203**, pp. 487-497

[12] N. Shao, W. Salman, A. Gavriilidis, P. Angeli, 2008, "CFD simulations of the effect of inlet conditions on Taylor flow formation", *International Journal of Heat and Fluid Flow,* **29**, pp. 1603-1611

[13] D. Liu, Sh. Wang, 2008, "Hydrodynamics of Taylor flow in noncircular capillaries", *Chemical Engineering and Processing,* **47**, pp. 2098-2106

[14] L. Wu, M. Tsutahara, L. Kim, M. Y. Ha, 2008, "Numerical simulations of droplet formation in a cross-junction microchannel by the lattice Boltzmann method", *International Journal for Numerical Methods in Fluids,* **57**, pp. 793-810

[15] Z. Yu, O. Hemminger, L.S. Fan, 2007, "Experiment and lattice Boltzmann simulation of two-phase gas-liquid flows in microchannels", *Chemical Engineering Science,* **62**, pp. 7172-7183

[16] D. Lakehal, G. Larrignon, Ch. Narayanan, 2008, "Computational heat transfer and two-phase flow topology in miniature tubes", *Microfluid Nanofluid,* **4**, pp. 261-271

[17] V. Kumar, S. Vashisth, Y. Hoarau, K.D.P. Nigam, 2007, "Slug flow in curved microreactors: Hydrodynamic study", *Chemical Engineering Science,* **62**, pp. 7494-7504
[18] B. E. Ghidersa, M. Worner, D. G. Cacuci, 2004, "Exploring the flow of immiscible fluids in a square vertical mini-channel by direct numerical simulation", *Chemical Engineering Journal,* **101**, pp. 285-294
[19] M. Muradoglu, A. Gunther, H. A. Stone, 2007, "A computational study of axial dispersion in segmented gas-liquid flow", *PHYSICS OD FLUIDS,* 19, 072109
[20] M. Worner, B. Ghidersa, A. Onea, 2007, "A model for the residence time distribution of bubble-train flow in a square mini-channel based on direct numerical simulation results", *International Journal of Heat and Fluid Flow,* **28**, pp. 83-94
[21] T. Taha, Z. F. Cui, 2006, "CFD modelling of slug flow in vertical tubes", *Chemical Engineering Science,* **61**, pp. 676-687
[22] T. Taha, Z.F. Cui, 2006, "CFD modelling of slug flow inside square capillaries", *Chemical Engineering Science,* **61**, pp. 665-675
[23] D. M. Fries, Ph. R. von Rohr, 2009, "Liquid mixing in gas-liquid two-phase flow by meandering microchannels", *Chemical Engineering Science,* **64**, pp. 1326-1335
[24] E. S. Baird, 2008, "Hydrodynamic and thermal modeling of two-dimensional microdroplet arrays for digitized heat transfer", *PhD Thesis, University of Colorado*
[25] P. Young, K. Mohseni, 2008, "The Effect of Droplet Length on Nusselt numbers in Digitized Heat Transfer", Proceedings of I-THERM, 2008, *11th IEEE Intersociety Conference on Thermal and Thermomechanical Phenomena in Electronic Systems*, pp. 352-359
[26] F. P. Bretherton, 1961, "The motion of long bubbles in tubes", *Journal of Fluid Mechanics,* **10**, pp. 166-188
[27] R. K. Edvinsson, S. Irandoust, 1996, "Finite-Element Analysis of Taylor Flow", *AIChE Journal,* **42** (7), pp. 1815-1823
[28] T. Taha, Z. F. Cui, 2004, "Hydrodynamics of slug flow inside capillaries", *Chemical Engineering Science,* **59**, pp. 1181-1190
[29] Q. He, K. Fukagata, N. Kasagi, 2007, "Numerical simulation of gas-liquid two-phase flow and heat transfer with dry-out in a micro tube", *6th International Conference on Multiphase flow, ICMF 2007,* Leipzig, Germany, July 9-13
[30] P. Ua-arayaporn, K. Fukagata, N. Kasagi, T. Himeno, 2005, "Numerical simulation of gas-liquid two-phase convective heat transfer in a micro tube", *ECI International Conference on Heat Transfer and Fluid Flow in Microscale,* Castelvecchio Pascoli, 25-30 September
[31] W. Salman, A. Gavriilidis, P. Angeli, 2004, "A model for predicting axial mixing during gas-liquid Taylor flow in microchannels at low Bodenstein numbers", *Chemical Engineering Journal,* **101**, pp. 391-396
[32] A. A. Armand, G. G. Treschev, 1946, "The resistance during the movement of a two-phase system in horizontal pipe", Izv. Vse. Teploket. Inst, Vol.1, pp. 16-23
[33] Ch. Narayanan, D. Lakehal, 2008, "Two-phase convective heat transfer in miniature pipes under normal and microgravity conditions", *Journal of Heat Transfer,* July 2008, Vol. 130
[34] F. Ilnicki, P. Sobieszuk, R. Pohorecki, 2009, "Simulations of a two phase flow in a closed microchannel", *Chemical and Process Engineering,* **30**, pp. 205-216
[35] A. Carlson, P. Kudinov, C. Narayanan, 2008, "Prediction of two-phase flow in small tubes: A systematic comparison of state-of-the-art CMFD codes", *5th European Thermal-Sciences Conference,* The Netherlands
[36] Ch. Chung, M. A. Hulsen, J. M. Kim, K. H. Ahn, S. J. Lee, 2008, "Numerical study on the effect of viscoelasticity on drop deformation in simple shear and 5:1:5 planar contraction/expantion microchannel", *Journal of Non-Newtonian Fluid Mechanics,* **155**, pp. 80-93
[37] M. N. Kashid, D. W. Agar, S. Turek, 2007, "CFD modeling of mass transfer with and without chemical reaction in the liquid-liquid slug flow microreactor", *Chemical Engineering Science*, **62**, pp. 5102-5109
[38] M. N. Kashid, I. Gerlach, S. Goetz, J. Franzke, J. F. Acker, F. Platte, D. W. Agar, S. Turek, 2005, "Internal circulation within the liquid slugs of a liquid-liquid slug-flow capillary microreactor", *Industrial & Engineering Chemistry Research,* **44**, pp. 5003-5010
[39] M. N. Kashid, D. F. Rivas, D. W. Agar, S. Turek, 2008, "On the hydrodynamics of liquid-liquid slug flow capillary microreactors", *ASIA-PACIFIC JOURNAL OF CHEMICAL ENGINEERING,* **3**, pp. 151-160
[40] A. Onea, M. Worner, D. G. Cacuci, 2009, "A qualitative computational study of mass transfer in upward bubble train flow through square and rectangular mini-channels", *Chemical Engineering Science,* **64**, pp. 1416-1435
[41] N. M. Raimondi, L. Part, Ch. Gourdon, P. Cognet, 2008, "Direct numerical simulations of mass transfer in square microchannels for liquid-liquid slug flow", *Chemical Engineering Science,* **63**, pp. 5522-5530
[42] S. N. Reznik, A. L. Yarin, 2002, "Strong squeezing flow between parallel plates leads to rolling motion at the contact line", *International Journal of Multiphase Flow,* **28**, pp. 911-925
[43] H. Oprins, J. Danneels, B. Van Ham, B. Vandevelde, M. Baelmans, 2008, "Convection heat transfer in electrostatic actuated liquid droplets for electronics cooling", *Microelectronics Journal,* **39**, pp. 966-974
[44] T. S. Sammarco, M. A. Burns, 2000, "Heat-transfer analysis of microfabricated thermocapillary pumping and reaction devices", *J. Micromech. Microeng.,* **10**, pp. 42-55
[45] L. Wu, M. Tsutahara, L. S. Kim, M.Y. Ha, 2008, "Three-dimensional lattice Boltzmann simulations of droplet formation in a cross-junction microchannel", *International Journal of Multiphase Flow,* **34**, pp. 852-864